



# Equilibrium Optimizer Based Fractional Order PID Control of Brushless DC Motor

Ali Temir<sup>1</sup>, Burhanettin Durmuş<sup>2\*</sup>

<sup>1</sup> Kütahya Dumlupınar University, Institute of Graduate Education, Graduate Student, Kütahya, Turkey, (ORCID: 0000-0001-6854-9575), [ali.tamr838@gmail.com](mailto:ali.tamr838@gmail.com)

<sup>2\*</sup> Kütahya Dumlupınar Üniversitesi, Faculty of Engineering, Department of Electrical and Electronics Engineering, Kütahya, Turkey, (ORCID: 0000-0002-8225-3313), [burhanettin.durmus@dpu.edu.tr](mailto:burhanettin.durmus@dpu.edu.tr)

(İlk Geliş Tarihi 27 Şubat 2023 ve Kabul Tarihi 17 Mayıs 2023)

(DOI: 10.31590/ejosat.1256908)

**ATIF/REFERENCE:** Temur, A. & Durmuş, B. (2023). Equilibrium Optimizer Based Fractional Order PID Control of Brushless DC Motor. *European Journal of Science and Technology*, (51), 153-161.

## Abstract

The main challenges of Proportional Integral Derivative (PID) control are sudden set-point changes and parameter changes, which leads to poor response. It can be taken into account that this control unit can be replaced by another similar control unit, but it differs from it in the degree of integration and differentiation, and this is what is known as Fractional-Order PID (FOPID), which improves the performance of the system in the transient state. To choose the FOPID constants, various methodologies, including optimization algorithms, are used to obtain the best possible performance. In this paper, the speed of brushless DC motor (BLDC) was regulated using (FOPID), where the equilibrium optimizer (EO) algorithm was used to find the values of the controller constants, and the performance of this algorithm was compared with several other optimization algorithms such as particle swarm optimization (PSO), differential evolution (DE), and golden jackal optimization (GJO). Simulation results in Matlab-Simulink 2016a showed the effectiveness of the proposed algorithm (EO) in achieving response time, overshoot, and lower steady state error compared with the rest of the algorithms.

**Keywords:** Equilibrium Optimizer, FOPID, PID, BLDC Motor.

## Fırçasız DC Motorun Denge Optimizasyon Algoritması Tabanlı Kesir Dereceli PID Kontrolü

### Öz

Oransal-İntegral-Türevsel (PID) kontrolün ana zorlukları, zayıf kontrol cevabına yol açan ani ayar noktası değişiklikleri ve parametre değişiklikleridir. Bu kontrol ünitesinin yerine Kesir Dereceli PID (FOPID) olarak bilinen benzer bir kontrol ünitesi kullanılabilir. Ancak FOPID 'nin integral ve türev dereceleri geleneksel PID'den farklıdır ve bu farklılık, geçici durumda sistemin performansını artırmaktadır. FOPID katsayılarının belirlenmesinde, mümkün olan en iyi performansı elde etmek için optimizasyon algoritmaları da dahil olmak üzere çeşitli metodolojiler kullanılmaktadır. Bu makalede, fırçasız DC motor (BLDC) hız kontrolü için FOPID tasarımı gerçekleştirilmiştir. Kontrolör parametrelerini belirlemek için Denge Optimizasyon Algoritması (EO) kullanılmış ve algoritmanın performansı, Parçacık Sürü Optimizasyonu (PSO), Farksal Gelişim (DE) ve Altın Çakal Optimizasyon (GJO) algoritmalarıyla karşılaştırılmıştır. Matlab-Simulink 2016a'daki simülasyon sonuçları, önerilen algoritmanın diğer algoritmalara kıyasla daha iyi tepki süresi, aşım ve daha düşük kararlı hal hatası elde etmedeki etkinliğini göstermektedir.

**Anahtar Kelimeler:** EO Algoritması, FOPID, PID, BLDC Motor.

\* Corresponding Author: [burhanettin.durmus@dpu.edu.tr](mailto:burhanettin.durmus@dpu.edu.tr)

## 1. Introduction

The science of electrical control engineering has witnessed rapid development in recent years, and the methodologies and techniques used in control systems have multiplied, and they vary and differ in their advantages and methods of implementation. Due to the proportional integral differential (PID) controller's simplicity, and simple tuning parameters, it has been widely employed in industrial applications (Denizci & Ulu, 2020; Köse & Oktay, 2020; El-Zohri and Mosbah, 2020; Singh et al., 2013; Najib et al., 2007).

With regard to the PID control unit, each part has a different effect on the quality and efficiency of the control system. For example, the response time can be reduced by increasing the proportional or integral constant, while the opposite is obtained in order to increase the differential constant. In order to overshoot, it increases by increasing the proportional or integral constant, while the opposite occurs in order to increase the differential constant, in order to reduce the steady-state error, the proportional constant can be increased, and it can be made equal to zero in the presence of the integral constant, while the effect of the differential constant is limited to the value of the steady-state error (Najib et al., 2007; Hannan et al., 2018).

In fact, the goal of the control system is to improve the performance and stability of the control system, including, reducing overshooting, response time, static error, and confronting system parameters' changes and external disturbances. The primary challenges for PID control technology are abrupt set point changes and parameter variations, which result in poor response, so it can be replaced by another controller that is similar, but differs from it in the degree of integration and differentiation, and this is what is known as fractional order PID (FOPID), which adds robustness and improves the performance of the system in the transient state (Euldji et al., 2022; Yang et al. 2019; Jamil et al., 2022).

FOPID control has gained a lot of traction and drawn increasing attention in several technical fields during the past 10 years, including electrical motor driving and robotics engineering (Euldji et al., 2022; Tepljakov et al., 2018; Xue et al., 2006). Compared to traditional PID control, tuning the FOPID controller's five parameters ( $K_P$ ,  $K_I$ ,  $K_D$ ,  $\lambda$ ,  $\mu$ ) is a difficult process. Different methodologies can be used for tuning the FOPID controller's five parameters, including adaptive control, fuzzy control, neural network and optimization algorithms, to obtain the best possible performance.

In the study, (Kumar et al., 2017), in addition to decreasing the initial overshoot, it has created a modified PID controller to track the desired speed with/without load, where the three terms of the controller are distributed, the integral term is used in the feed-forward path while the terms proportional and derivation are used in the feedback path. Both controllers were able to achieve a steady state error of zero; however the disadvantage of the standard PID may be seen in its pronounced overshoot during transient responses.

Three robust controller strategies for brushless DC motors (BLDC) are presented in paper (Shamseldin and El-Samahy, 2014). These techniques include a self-tuning fuzzy PID controller, a genetic algorithm for modifying PID controller parameters, and a standard PID controller. The suggested controllers were compared in order to maintain the intended speed despite parameter fluctuations and outside disturbances. The suggested self-tuning fuzzy PID controller performs better, according to the simulation results.

The paper (Euldji et al., 2022) looks at a design for an optimal backstepping fractional order PID controller to handle the wheeled mobile robots (WMR) trajectory tracking problem. Parameter tuning has been done using a hybrid meta-heuristic optimization technique. The original algorithms The particle swarm optimization (PSO), grey wolf optimization (GWO), whale optimization algorithm (WOA), and a hybrid algorithm for scientific workflow scheduling in cloud computing (HPSOGWO) are contrasted with the efficiency of the hybrid WGO (HWGO) algorithm. The recommended HWGO methodology had the maximum efficiency among the other techniques in terms of settling and rising time, overshoot, and steady-state error, according to the simulation results in the MATLAB-Simulink.

The other paper (Xue et al., 2006) investigates a fractional order PID controller for a DC motor position control system. Numerous simulation comparisons in this work show that the fractional order PID controller will perform better than the traditional integer order PID controller provided it is designed and implemented appropriately.

In this work, FOPID controller is designed for BLDC motor speed control. FOPID coefficients were estimated with metaheuristic algorithms equilibrium optimizer (EO), golden jackal optimization (GJO), differential evolution (DE), and particle swarm optimization (PSO). Obtained results overshoot, rise time and errors were compared.

## 2. BLDC Motor

Electric motors are machines that convert electrical energy into mechanical motion. In our current era, the use of electric motors has become inevitable with their appearance in an unlimited number of applications, starting with household applications (refrigerators, washing machines, fans i.e) and commercial applications (heating, ventilation, air conditioning i.e) up to industrial applications (actuators, production lines i.e).

Brushless DC motors are considered one of the classes of synchronous motors, in which magnets are installed on the rotating part (and therefore called permanent magnetic motors), while the excitation coils are placed on the stator. Brushless DC motors (BLDC) are spreading very quickly, as they have many important advantages, they are highly dynamic, less noise, and do not require much maintenance as in the case of brushed DC motors, the relationship between current and torque is linear, they have speed versus torque characteristics better than DC motor and they have a torque-to-volume ratio that makes them suitable for applications that take into account size and weight (Shamseldin and El-Samahy, 2014; Lavanya et al., 2015).

The BLDC motor is normally fed via a three-phase inverter consisting of two MOSFET/diode switches connected to a constant DC source. The work of the inverter depends on the pulses coming from the control unit on the one hand, and on the signals of the Hall sensors that determine the position of the rotor on the other hand (Shamseldin and El-Samahy, 2014; Lavanya et al., 2015).

Figure 1 shows the equivalent circuit for a star-connected three-phase motor.

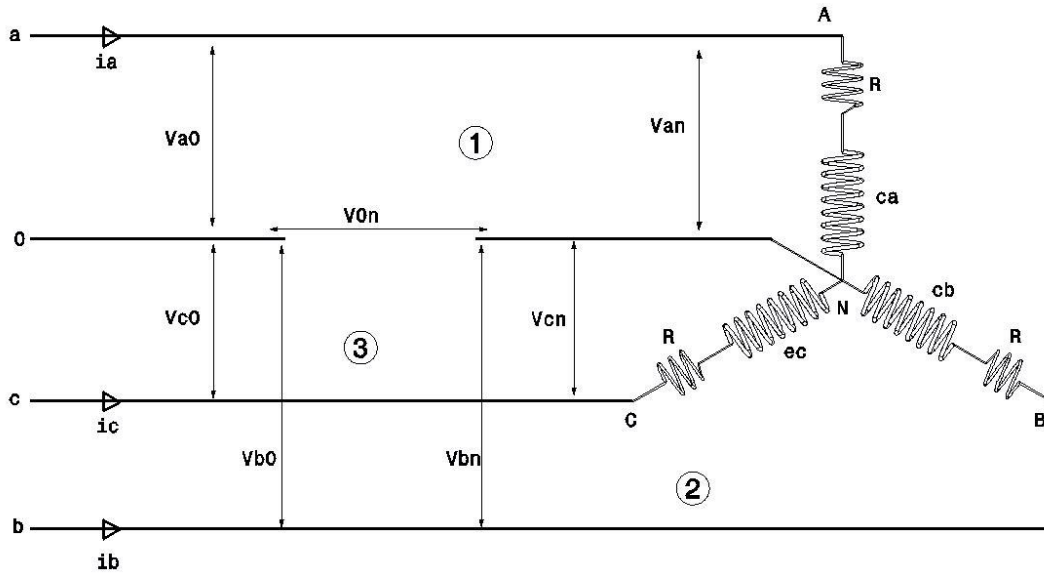


Figure 1. Equivalent circuit of a three-phase motor

According to Kirchhoff's voltage law, the following voltage equations can be obtained (Shamseldin and El-Samahy, 2014; Lavanya et al., 2015):

$$V_{a0} - V_{n0} = Ri_a + L \frac{d}{dt}(i_a) + e_a \quad (1)$$

$$V_{b0} - V_{n0} = Ri_b + L \frac{d}{dt}(i_b) + e_b \quad (2)$$

$$V_{c0} - V_{n0} = Ri_c + L \frac{d}{dt}(i_c) + e_c \quad (3)$$

Where R is stator coil resistance, L is stator coil inductance, and e is the back electromotive force.

$$e_a = k_{fi} \cdot \omega_m \cdot F(\theta) \quad (4)$$

$$e_b = k_{fi} \cdot \omega_m \cdot F\left(\theta - \frac{2\pi}{3}\right) \quad (5)$$

$$e_c = k_{fi} \cdot \omega_m \cdot F\left(\theta - \frac{4\pi}{3}\right) \quad (6)$$

Where  $k_{fi}$  is the back-emf constant,  $\omega_m$  is the rotor angular speed, and  $F(\theta)$  is a trapezoidal shape function which is given as follows:

$$F(\theta) = \begin{cases} \left(\frac{6}{\pi}\right)\theta, & (0 < \theta \leq \pi/6) \\ 1, & (\pi/6 < \theta \leq 5\pi/6) \\ -\left(\frac{6}{\pi}\right)\theta + 6, & (5\pi/6 < \theta \leq 7\pi/6) \\ -1, & (7\pi/6 < \theta \leq 11\pi/6) \\ \left(\frac{6}{\pi}\right)\theta + 12, & (11\pi/6 < \theta \leq 2\pi) \end{cases}$$

Fixing the equations 1, 2 and 3, we get

$$V_{n0} = \frac{1}{3} [(V_{a0} + V_{b0} + V_{c0}) - (e_a + e_b + e_c)] \quad (7)$$

As a result of the motor rotation, the motion's equation is given as follow:

$$T_e - T_L = f\omega_m + J \frac{d\omega_m}{dt} \quad (8)$$

$T_L$  is the load torque, J is the rotary inertia, f is the damping coefficient,  $T_e$  is the electromagnetic torque which is given as follows:

$$T_e = K_{fi} \left[ F(\theta)i_a + F\left(\theta - \frac{2\pi}{3}\right)i_b + F\left(\theta - \frac{4\pi}{3}\right)i_c \right] \quad (9)$$

As the BLDC motor parameters are given in Table 1.

Table 1. BLDC motor parameters

| Symbol   | Parameter           | Value                     |
|----------|---------------------|---------------------------|
| $k_{fi}$ | Torque constant     | 0.0193 N.m/A              |
| $R$      | Stator resistance   | 0.3240 $\Omega$           |
| $L$      | Stator inductance   | 0.2715 e-3 H              |
| $B$      | Friction constant   | 4 e-5 N.m.sec/rad         |
| $J$      | Inertia torque      | 1.2 e-5 kg.m <sup>2</sup> |
| $P$      | The number of poles | 4                         |
| $n$      | Rotor speed         | 4770 rpm                  |
| $V_{dc}$ | Stator Voltage      | 24 V                      |
| $T_L$    | Load torque         | 0.1 N.M                   |

### 3. Equilibrium optimizer (EO)

The Equilibrium Optimizer (EO) is an optimization algorithm which is used to predict both dynamic and equilibrium states and was inspired by control volume mass balance models. Every particle (solution) in EO, along with its concentration and location, functions as a search engine. To eventually arrive at the equilibrium state, the search agents update their concentration at random with regard to the best solutions, or equilibrium candidates (optimal result). It had been demonstrated that a clearly defined "generation rate" term enhances EO's capacity for exploration, exploitation, and local minima evasion (Faramarzi et al., 2020; Houssein et al., 2021; Dubey et al., 2021).

The equation that specifies the mass conservation process that enters and exits a particular volume, where the system constantly tends to equilibrium point, is the foundation of the EO algorithm. In fact, the algorithm makes an effort to keep the system's concentration stable.

The first-order differential equation that describes how mass entering and mass exiting a dynamic system are related is written as follows:

$$V \frac{dc}{dt} = Q \cdot C_{eq} - Q \cdot C + g \quad (10)$$

Where,  $C$  is the volume concentration,

$V \frac{dc}{dt}$  is the rate at which mass changes,

$Q$  is the flow rate,

$C_{eq}$  is the concentration when it reaches equilibrium,

$g$ . is the rate of mass generation.

When it hits 0, the equilibrium state is intended to be reached. The derivative can be solved as a function of where and called the turnover rate.

We may rearrange and rewrite equation (10) as

$$\frac{dc}{\lambda \cdot C_{eq} - \lambda \cdot C + \frac{g}{V}} = dt \quad (11)$$

and

$$\int_{c_0}^c \left( \frac{dc}{\lambda \cdot C_{eq} - \lambda \cdot C + \frac{g}{V}} \right) = \int_{t_0}^t dt \quad (12)$$

After rearranging and integrating, the final concentration update equation is:

$$C = C_{eq} + (C_0 - C_{eq}) \cdot F + \frac{g}{\lambda \cdot V} (1 - F) \quad (13)$$

Where

$$F = \exp[-\lambda(t - t_0)] \quad (14)$$

During the EO optimization process, equation (13) offers the methodology for locating an optimal solution.  $C_{eq}$  is a solution that was chosen at random from a pool of the top 3 to 5 solutions after the issue was solved under various situations. The difference between a solution's location and the equilibrium state chosen at random makes up the second term  $(C_0 - C_{eq})$ . This term offers direct search, induces particles to do a global search, and effectively and thoroughly explore the solution space. The third term  $\left\{ \frac{g}{\lambda \cdot V} (1 - F) \right\}$  is associated with rate both generation and turnover. This phrase updates/improves the solution by exploitation; as a consequence, the stages are brief, leading to minute adjustments to fine-tune the answer; occasionally, though, it permits exploration.

The optimization procedure is carried out by the EO algorithm in five phases, which are listed below.

*Initialization:*

The initialization process in EO is like metaheuristics based on population. By creating concentrations at random that are between the lower and upper bounds for each vector dimension, the starting population is produced. To build the  $i$ th population vector, it can be use the following equation:

$$c_i^{initial} = rand(particles\ no, 1) * (ub_i - lb_i) + lb_i \quad (15)$$

Here,  $C_{max}$  and  $C_{min}$  stand for vectors that indicate the upper and lower concentrations of the various solution vector dimensions. The evaluated created solutions are assessed to establish their fitness value. The equilibrium pool is then created using the top three to five solutions.

*Equilibrium Pool and Candidates:*

The equilibrium state, which is attained after convergence, is the problem's optimal overall solution. The best answers from runs completed under various conditions are stored in the equilibrium pool. Additionally, as illustrated, the pool contains the arithmetic mean of these top solutions:

$$\vec{C}_{eq,pool} = \{\vec{C}_{eq,1}, \vec{C}_{eq,2}, \vec{C}_{eq,3}, \vec{C}_{eq,4}, \vec{C}_{eq,ave}\} \quad (16)$$

One of these top answers from (16) is randomly chosen to update the location of a particle using (13). For every equilibrium concentration of the pool, the chance of selection is the same. Let's say there are the 5 potential answers indicated above. If any of the first four equilibrium states or solutions in the pool is chosen for the position update mechanism, the new solution will then be produced through exploration. On the other side, exploitation is done to create a new solution or state if the fifth candidate is selected for position update.

*Exponential Term:*

The exponential term ( $\mathcal{F}$ ) is the third component in Equation (13), which updates the concentration. This phrase aims to effectively balance exploitation and exploration in the EO algorithm.

$$F = \exp[-\lambda(t - t_0)] \quad (17)$$

The turnover rate ( $\lambda$ ) is a number generated at random between 0 and 1. Time is symbolized by the constant  $t$ , which gets smaller with each iteration, as seen below.

$$t = \left(1 - \frac{iter}{Max\ iter}\right)^{a2 * \frac{iter}{Max\ iter}} \quad (18)$$

$$\vec{t}_0 = \frac{1}{\lambda} \ln \{-a_1 \cdot sign(r - 0.5[1 - e^{-\lambda t}] + t)\} \quad (19)$$

The ultimate formula for the exponential term ( $\mathcal{F}$ ) shown in Equation (20) is obtained by substituting (19) into (17). For all four combination scenarios, it can be observed that the exponential term ( $\mathcal{F}$ ) variation with iteration decreases (in both directions) and eventually converges to zero. The type of variation reveals the term's efficacy in carrying out exploration and exploitation.

$$\vec{F} = a_1 \cdot sign(r - 0,5)[e^{-\lambda t} - 1] \quad (20)$$

The variables  $a_1$  and  $a_2$  in EO control exploration and exploitation, respectively. In addition to these two, the term  $sign(r - 0,5)$  influences the search's direction of exploration and exploitation.

*Generation Rate:*

This term includes the third factor in the concentration updating equation provided by (13). The generation rate guarantees that the algorithm will reach the best overall solution ( $\vec{g}$ ), which makes the convergence process more streamlined by fine-tuning the solutions with brief updates. The generation rate can be specified ( $\vec{g}$ ) as

$$\vec{g} = \vec{g}_0 \cdot e^{-\lambda(t-t_0)} = \vec{g}_0 \cdot \vec{F} \quad (21)$$

$$\vec{g}_0 = GCP(\vec{C}_{eq} - \lambda \cdot \vec{C}) \quad (22)$$

The generation rate constants ( $GCP$ ) determines how the generation rate factor will be used to update the particle location in the (13). This option is intended to govern how the particle is used and explored in the following ways:

$$GCP = \begin{cases} 0.5r1 & r2 > p \\ 0 & r1 < p \end{cases} \quad (22)$$

The generation probability represented by ( $p$ ) also determines the likelihood that the particle will use the generation rate term whereas updating its concentration by (13). Here, the random integers  $[0, 1]$  are dispersed evenly between  $r1$  and  $r2$ . The generation rate parameter and update step size will both be tiny if the first condition in equation (22) is true, leading to exploitation.

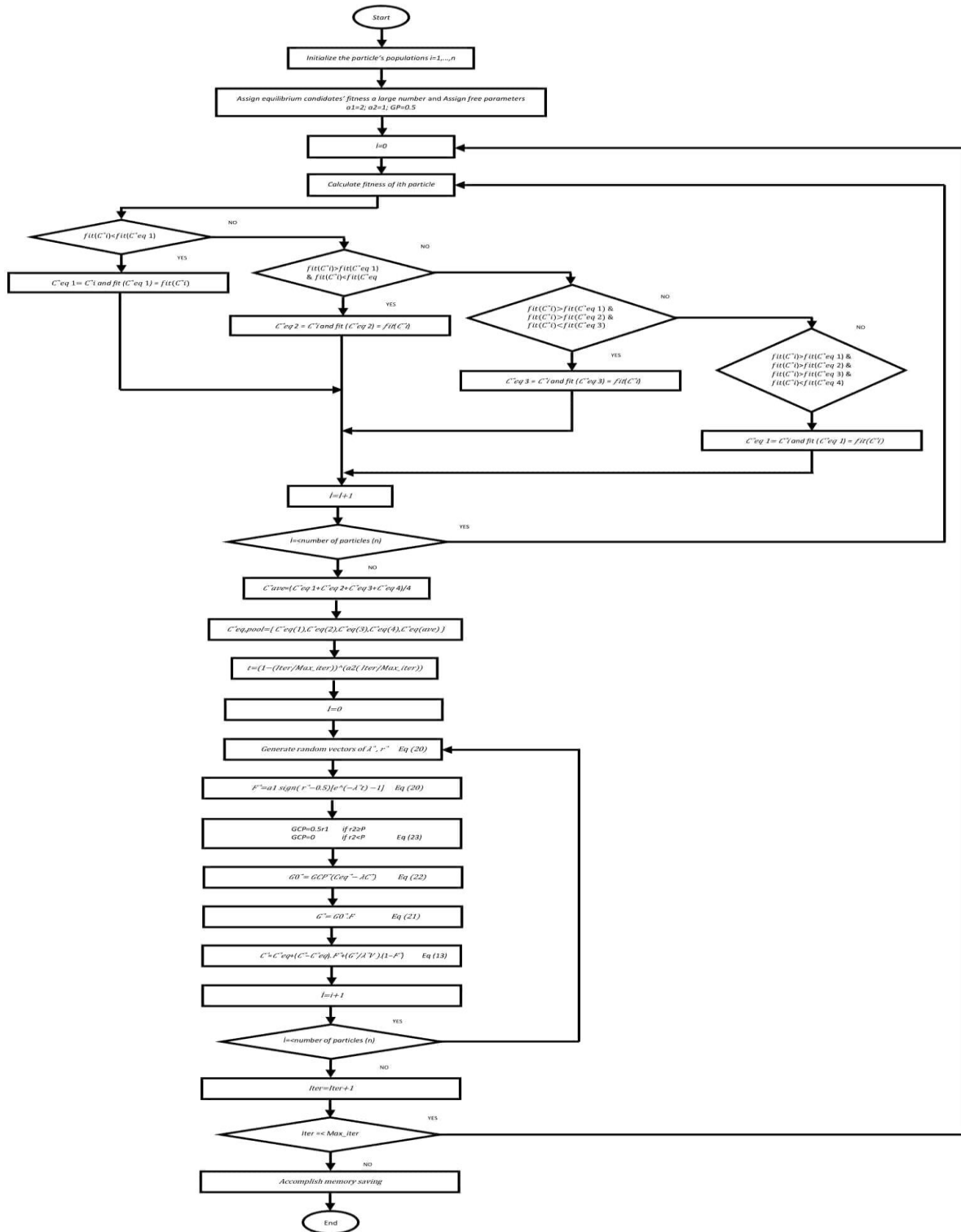


Figure 2. The flowchart of EO algorithm

However, if the second condition holds true, ( $GCP$ ) and ( $g$ ) both become zero, therefore the particle is updated without any input from the generation rate term. According to experiments, the search is balanced between exploitation and exploration when ( $p$ ) is set at 0.5. Exploration is seen to rise when generation probability ( $p$ ) is raised above 0.5, and exploitation is seen to increase as ( $p$ ) is lowered below 0.5.

Particle's Memory Saving:

To prevent losing a superior solution throughout the process, some sort of memory mechanism must be implemented in metaheuristic algorithms. The best location and associated fitness of each particle in EO are also saved and updated if there is an

improvement in following iterations, in a manner much resembling the pbest in PSO. The flowchart of EO algorithm is given in Figure 2.

### 4. Simulation Results

The simulation as shown in Figure 3 is carried out using MATLAB/SIMULINK. The Simulink block consists of 3-phase star connected BLDC motor, 3-phase VSI, PWM block, and speed FOPID controller, where Figure 4 shows the structure of this controller.

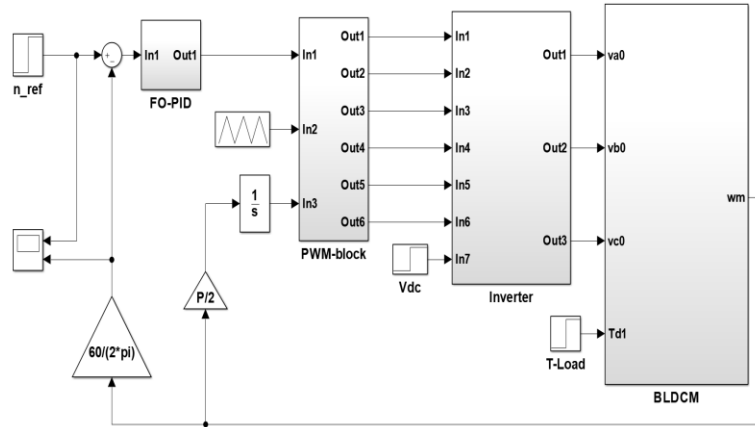


Figure 3. The simulink model of FOPID control of BLDC motor

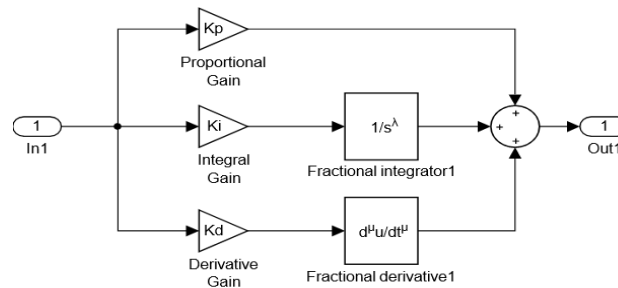


Figure 4. The structure of FOPID controller

The speed reference value is set at 4770 rpm, with load torque applied (0.1 N.m) in time 0.025 sec, as shown in Figure 5, while Figure 6 shows the current drawn on the first phase of the motor. Figure 7 shows the speed response for different optimization algorithms for adjusting the FOPID controller parameters and Figure 8 shows zoom in for the Figure 7.

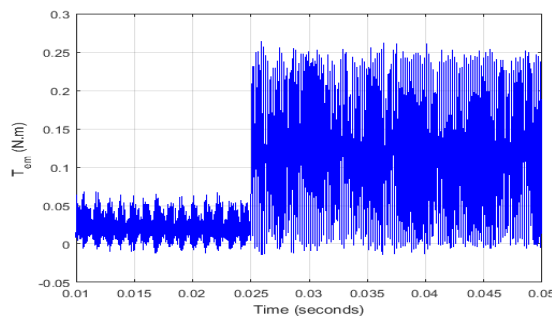


Figure 5. Electromagnetic torque of the motor



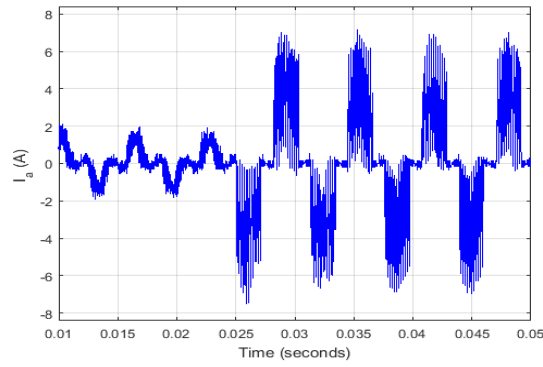


Figure 6. The current drawn on the motor's first phase

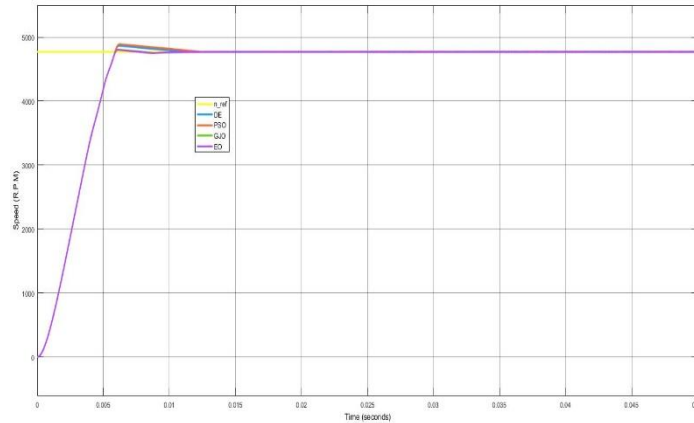


Figure 7. The speed responses of optimization algorithms

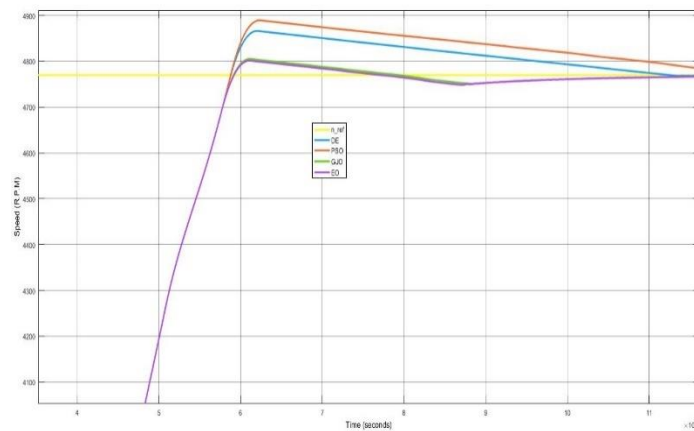


Figure 8. Zoomed speed responses of optimization algorithms

As can be seen from the Figure 6, the current has an almost sinusoidal shape (trapezoidal shape) with an amplitude equal to 2 A when the load torque is equal to zero, while the amplitude becomes 7 A after applying the load torque at the moment (0.025sec), as it is noted from the Figure 5 that the value of the electromagnetic moment increased from 0.025N.m to 0.125N.m at this moment.

It is noted from figures 7 and 8 that the performance of the EO algorithm is the best compared to the rest of the algorithms. The EO algorithm converges to the target speed faster than other algorithms. In other words, its convergence performance is better than the others. Thus, it follows the target speed more closely. Also, from Table 2, the performance of EO algorithm is better than others in terms of overshoot, settling time and steady state error. The proposed method provides the lowest *ITAE* value of 0.02921.

Table 2. Optimized FOPID controller parameters and performance of various algorithms

| Optimum parameters | PSO   | DE      | GJO      | EO       |
|--------------------|-------|---------|----------|----------|
| $K_P$              | 100   | 21.7458 | 67.97280 | 65.2798  |
| $K_I$              | 0.001 | 0.010   | 5.370026 | 4.687011 |
| $K_D$              | 0.001 | 0.001   | 0.014443 | 0.013605 |
| $\lambda$          | 0.001 | 0.3399  | 0.888543 | 0.876854 |



|          |         |         |          |          |
|----------|---------|---------|----------|----------|
| $\mu$    | 0.001   | 0.900   | 0.895182 | 0.899825 |
| ITAE     | 0.03217 | 0.03141 | 0.02924  | 0.02921  |
| TS (sec) | 0.0123  | 0.0116  | 0.0114   | 0.0113   |
| Mp (%)   | 2.43    | 2.03    | 0.68     | 0.67     |

## 5. Conclusions

In this paper, an adaptive FOPID controller is designed for DC motor speed control. The motor speed was regulated using the proportional-integral- differential fractional controller, where a comparative study was conducted between several algorithms to set the constants of the controller, which are: PSO, DE, GJO and EO.

The simulation results in MATLAB-Simulink showed the efficiency of the EO algorithm as it had an ITAE less than PSO by 10%, DE by 7.5%, GJO by 0.1%. It has a higher response speed, as its settling time is lower than PSO by 8.8%, DE by 2.6%, and GJO by 0.88%. It also has a lower overshoot rate than PSO by 262%, DE by 200%, GJO by 1.5%. Hence, the proposed algorithm is superior and effective than those compared methods. It is a promising approach to solving other real-world engineering problems.

## References

- Denizci, A., & Ulu, C. (2020). Fuzzy Cognitive Map Based PID Controller Design. *European Journal of Science and Technology, Special Issue*, 165-171.
- Dubey, S. M., Dubey, H. M., Pandit, M., & Salkuti, S. R. (2021). Multiobjective Scheduling of Hybrid Renewable Energy System Using Equilibrium Optimization. *Energies*, 14 (19), 6376.
- El-Zohri, E. H., & Mosbah, M. A. (2020, February). Speed control of inverter-fed induction motor using hybrid fuzzy-PI controller. In *2020 International Conference on Innovative Trends in Communication and Computer Engineering (ITCE)*, Aswan, Egypt, 216-221.
- Euldji, R., Batel, N., Redha, R., Noureddine K., et al. (2022). Optimal Backstepping-FOPID Controller Design for Wheeled Mobile Robot. *Journal Europeen des Systemes Automatises*, 55 (1), 97-107.
- Faramarzi, A., Heidarinejad, M., Stephens, B., & Mirjalili, S. (2020). Equilibrium Optimizer: A Novel Optimization Algorithm. *Knowledge-Based Systems*, 191, 105190.
- Hannan, M. A., Abd Ali, J., Ker, P. J., Mohamed, A., Lipu, M. S., & Hussain, A. (2018). Switching Techniques and Intelligent Controllers for Induction Motor Drive: Issues and Recommendations. *IEEE Access*, 6, 47489-47510.
- Houssein, E. H., Nageh, G., Abd Elaziz, M., & Younis, E. (2021). An Efficient Equilibrium Optimizer for Parameters Identification of Photovoltaic Modules. *PeerJ Computer Science*, 9 (7), e708.
- Jamil, A. A., Tu, W. F., Ali, S. W., Terriche, Y., & Guerrero, J. M. (2022). Fractional-Order PID Controllers for Temperature Control: A Review. *Energies*, 15 (10), 3800.
- Köse, O., & Oktay, T. (2020). Investigation of the Effect of Differential Morphing on Lateral Flight by Using PID Algorithm in Quadrotors. *European Journal of Science and Technology*, 18, 636-644.
- Kumar, B., Swain, S. K., & Neogi, N. (2017). Controller Design for Closed Loop Speed Control of BLDC Motor. *International Journal on Electrical Engineering and Informatics*, 9 (1), 146-160.
- Lavanya, Y., Bhavani, N. P. G., Ramesh, N., & Sujatha, K. (2015). Sensorless Vector Control of BLDC using Extended Kalman Filter. *Signal & Image Processing: An International Journal (SIPIJ)*, 6 (3), 103-114.
- Najib, M. S., Jadin, M. S., Ismail, R. M. T. R., & Mohamed, M. R. (2007, October). Design and Implementation of PID Controller in Programmable Logic Controller for DC Motor Position Control of the Conveyor System. In *Proceedings of the 3rd WSEAS/IASME International Conference on Dynamical Systems and Control*, Arcachon, France, 266-270.
- Shamseldin, M. A., & EL-Samahy, A. A. (2014, September). Speed Control of BLDC Motor by using PID Control and Self-Tuning Fuzzy PID Controller. In *15th International Workshop on Research and Education in Mechatronics (REM)*, El Gouna, Egypt, 1-9.
- Singh, A. P., Narayan, U., & Verma, A. (2013). Speed Control of DC Motor using PID Controller Based on Matlab. *Innovative Systems Design and Engineering*, 4 (6), 22-28.
- Tepljakov, A., Alagoz, B. B., Yeroglu, C., Gonzalez, E., HosseinNia, S. H., & Petlenkov, E. (2018). FOPID Controllers and Their Industrial Applications: A Survey of Recent Results. *IFAC-PapersOnLine*, 51 (4), 25-30.
- Xue, D., Zhao, C., & Chen, Y. (2006, June). Fractional order PID Control of a DC-Motor with Elastic Shaft: A Case Study. In *2006 American Control Conference*, Minnesota, USA, 3182-3187.
- Yang, B., Yu, T., Shu, H., Han, Y., Cao, P., & Jiang, L. (2019). Adaptive Fractional Order PID Control of PMSG based Wind Energy Conversion System for MPPT using Linear Observers. *International Transactions on Electrical Energy Systems*, 29 (1), e2697.